

# A biologically inspired two-species exclusion model: effects of RNA polymerase motor traffic on simultaneous DNA replication

Soumendu Ghosh,<sup>1</sup> Bhavya Mishra,<sup>1</sup> Shubhadeep Patra,<sup>2</sup> Andreas Schadschneider,<sup>3</sup> and Debashish Chowdhury<sup>1</sup>

<sup>1</sup>*Department of Physics, Indian Institute of Technology Kanpur, 208016, India*

<sup>2</sup>*ISERC, Visva-Bharati, Shantiniketan 731235, India*

<sup>3</sup>*Institute for Theoretical Physics, University of Cologne, Köln, Germany*

We introduce a two-species exclusion model to describe the key features of the conflict between the RNA polymerase (RNAP) motor traffic, engaged in the transcription of a segment of DNA, concomitant with the progress of two DNA replication forks on the same DNA segment. One of the species of particles ( $P$ ) represents RNAP motors while the other ( $R$ ) represents replication forks. Motivated by the biological phenomena that this model is intended to capture, a maximum of only two  $R$  particles are allowed to enter the lattice from two opposite ends whereas the unrestricted number of  $P$  particles constitute a totally asymmetric simple exclusion process (TASEP) in a segment in the middle of the lattice. Consequently, the lattice consists of three segments; the encounters of the  $P$  particles with the  $R$  particles are confined within the middle segment (segment 2) whereas only the  $R$  particles can occupy the sites in the segments 1 and 3. The model captures three distinct pathways for resolving the co-directional as well as head-collision between the  $P$  and  $R$  particles. Using Monte Carlo simulations and heuristic analytical arguments that combine exact results for the TASEP with mean-field approximations, we predict the possible outcomes of the conflict between the traffic of RNAP motors ( $P$  particles engaged in transcription) and the replication forks ( $R$  particles). The outcomes, of course, depend on the dynamical phase of the TASEP of  $P$  particles. In principle, the model can be adapted to the experimental conditions to account for the data quantitatively.

## I. INTRODUCTION

The totally asymmetric simple exclusion process (TASEP) [1–4] was originally introduced as a simplified model describing the kinetics of protein synthesis [5, 6]. Since then it has found many more applications to biological systems, especially to situations [7–26], where the kinetics is dominated by the traffic-like collective motion of molecular motors (for reviews, see [27–31]). Genetic message encoded chemically in the sequence of the monomeric subunits of DNA is transcribed into an RNA molecule by a molecular motor called RNA polymerase (RNAP). In each of its step on the DNA track a RNAP motor elongates the nascent RNA molecule by a single subunit using the same DNA strand as the corresponding template [32]. TASEP-based models have also been developed for the traffic-like collective movements of RNAP motors on the same segment of DNA while each RNAP synthesizes a distinct copy of the same RNA [33–38].

A segment of DNA can undergo multiple rounds of transcription during the lifetime of a cell. In contrast, each DNA molecule is replicated once, and only once, just before the cell divides into two daughter cells [32]. A molecular machine called DNA polymerase (DNAP) is a key component of a replisome which is a multi-machine macromolecular complex that replicates DNA. As the replisomes unzip a duplex DNA and replicate the two exposed strands, Y-shaped junctions called replication forks, are formed. The progress of replication can be described in terms of the movement of two replication forks; replication of a segment of DNA is completed when two replication forks, approaching each other from opposite ends of the segment, collide head-on [32]. Theoretic-

cal models for the “nucleation” of replication competent replication forks and growth of the replicated domains of the DNA have been reported in the past [39–45] (see also [46, 47] for reviews).

Interestingly, transcription and replication can occur simultaneously on the same segment of DNA. However, typically, at a time only one of the two DNA strands of the DNA undergoes transcription by a traffic of RNAPs while both the strands are simultaneously replicated by distinct replisomes. Obviously, head-on collisions between a replication fork and RNAP motors is possible. Moreover, since the rate of replication is 10-20 times faster than that of transcription, a replication fork can catch up with a RNAP from behind thereby causing co-directional collision. Both types of collisions can have disastrous consequences [48], unless the transcription-replication conflict is resolved sufficiently rapidly to ensure maintenance of genomic stability. Nature has adopted multiple mechanisms of resolution of such conflict [49–52]. However, to our knowledge, no quantitative theoretical model of transcription-replication conflict and their resolution has been reported so far.

Here we propose a TASEP-based minimal model that captures the essential aspects of RNAP traffic on a segment of DNA concomitant with the progress of DNA replication forks from the two ends of the same DNA segment. The kinetics of the model incorporates all the known natural mechanisms of resolution of conflicts between DNA replication and transcription. This formulation, as explained in the next section, leads to a two-species exclusion process on a 3-segment lattice in one dimension which also includes “Langmuir kinetics”, i.e.

attachment and detachment of particles in the bulk [53]. One of the two species of particles represents RNAP motors all of which move co-directionally, i.e., say, from left to right. In contrast, only two particles of the second species, each representing a DNA replication fork, approach each other from opposite ends of the same track, i.e., one from the left and the other from the right. Because of the decrease of the separation between the two replication forks with the passage of time, the spatial region of conflict between the two species of particles also keeps shrinking. Thus, the model of the two-species exclusion process developed here is highly non-trivial.

By a combination of analytical arguments and computer simulations, we investigate the effect of the two processes, i.e., transcription and replication, on each other. More specifically, we indicate (a) the trends of variation of the mean time for completion of replication and (ii) the statistics of the successful and unsuccessful replication events, in the different phases of the RNAP traffic [2–4].

## II. MODEL

The schematic diagram of the model is shown in Fig. 1. For simplicity, motion of both species of particles are assumed to occur along a single common track represented by a one dimensional lattice of total length  $L$ , where,  $L$  is the total number of equispaced sites on the lattice. The lattice consists of three segments: sites  $i = 1$  to  $i = L_1 - 1$  (segment 1),  $i = L_1$  to  $i = L_2$  (segment 2), and site  $i = L_2 + 1$  to  $i = L$  (segment 3).

One of the two species of particles, labelled by  $P$ , represent the RNAP motors; all the  $P$  particles can move, by convention, only from left to right, i.e., from  $i$  to  $i + 1$ . There is no restriction on the number of  $P$  particles that can populate the lattice, except the limits arising naturally from the rates of entry, exit and forward hopping that are described below. In contrast, not more than two particles of the second species, labelled  $R$  and representing the replication forks, can ever enter the lattice irrespective of the kinetic rates, i.e., probabilities per unit time of the various kinetic processes that are described below. One of the  $R$  particles, denoted by  $R_\ell$  moves from left to right ( $i$  to  $i + 1$ ) whereas the other, denoted by  $R_r$  moves from right to left ( $i + 1$  to  $i$ ) on the lattice.

The  $R_\ell$  particle can enter the lattice only at  $i = 1$  with the probability  $\gamma$  per unit time. Similarly, the particle  $R_r$  can enter the lattice only at  $i = L$  with the probability  $\delta$  per unit time. After entry, the particles  $R_\ell$  and  $R_r$  can hop to the next site in their respective pre-determined directions of motion with the rates  $B_1$  and  $B_2$ , respectively (see Fig. 1). Both these particles can continue hopping, obeying the exclusion principles and rules of resolution of encounter with  $P$  particles as described below, till they encounter each other head-on at two nearest-neighbor sites on the lattice indicating completion of replication.

Unlike the  $R$  particles, all the  $P$  particles can enter the lattice only at the site  $i = L_1$  with the attachment rate (i.e., probability per unit time)  $\alpha_q$  provided that site is not already occupied by any other particle of either species. Once entered, a  $P$  particle can hop forward to the next site with the rate  $q$  if, and only if, the target site is not already occupied by any other  $P$  or  $R$  particle. A  $P$  particle can continue forward hopping, obeying the exclusion principle and the rules of resolution of encounter with  $R$  particles, till it reaches the site  $i = L_2$  from where it can exit with the rate  $\beta_q$ .

Thus, the division of lattice into three segments is based on the scenario that the lattice sites in the segments 1 and 3 can be occupied exclusively by only the  $R$  particles whereas the sites in middle region (i.e. segment 2) can get populated by both the  $P$  and  $R$  particles. However, in the segment 2 the  $P$  particles encounter the  $R_\ell$  particle co-directionally and  $R_r$  particle head-on. The final encounter between the two  $R$  particles, when they meet each other at two nearest-neighbour sites, is head-on.

Next we described the kinetics of both types of particles in the segment 2 which capture the mutual exclusion of the RNAP motors as well as the rules of resolution of the conflicts between transcription and replication. Mutual exclusion is captured by the simple rule that no site can be occupied simultaneously by more than one particle irrespective of the species to which it belongs. The three possible outcomes of the encounter between a  $P$  particle at the site  $i$  and a  $R_\ell$  particle at site  $i - 1$  or a  $R_r$  particle at the site  $i + 1$  are as follows:

- (a) The  $R$  particle can bypass the  $P$  particle with the rates  $p_{co}$  and  $p_{contra}$ , in the cases of co-directional and contra-directional encounter respectively, without dislodging the latter from the lattice and, therefore, both the particles can continue hopping in their respective natural direction of movement after the encounter.
- (b) The  $R$  particle can knock the  $P$  particle out of the track, with the rate  $D$  irrespective of the direction (co- or contra-directional) encounter and it resumes its hopping after the  $P$  particle is swept out of its way thereby aborting the transcription by that  $P$  particle prematurely.
- (c) Upon encounter with  $P$  particles, a  $R$  particle does not necessarily always win. In such situations, occasionally, the  $R$  particle detaches from the lattice with a probability  $C$  per unit time irrespective of the direction of encounter; this scenario captures the possible collapse of the replication fork that can causes genome instability. Once the replication fork collapses, the victorious  $P$  particle(s) resume their onward journey on the lattice.

If the  $R$  particles, entered from the sites  $i = 1$  and  $i = L$ , eventually meet each other on a pair of nearest-neighbour sites of the lattice, thereby indicating completion of the replication of the entire stretch of DNA from  $i = 1$  to  $i = L$ , we identify it as a successful event of type 1 (from now onwards we referred to it to as sr1). On the other hand, if one of the  $R$  particle stalls or collapses at any site in between  $L_1$  and  $L_2$  while the other

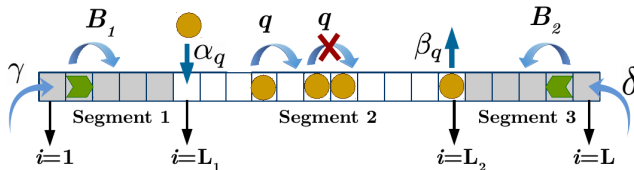


FIG. 1. A schematic diagram of the model. The whole lattice is divided into three segments  $\{1, 2, \dots, L_1 - 1\}$ ,  $\{L_1, \dots, L_2\}$  and  $\{L_2, \dots, L\}$ . A  $R$  particle (green arrow) can enter, either from the first site of segment 1 (i.e.  $i = 1$ ) with the probability  $\gamma$  per unit time or from the last site of segment 3 (i.e.  $i = L$ ), with the probability  $\delta$  per unit time. A  $R$  particle that enters through  $i = 1$  is allowed to hop from left to right (i.e.  $i \rightarrow i + 1$ ) with rate  $B_1$ , if the target site is empty. But, if a  $R$  particle enters through  $i = L$  it is allowed to hop only from right to left (i.e.  $i \rightarrow i - 1$ ), with rate  $B_2$ . Both the  $R$  particles continue their motion until they meet each other, at a pair of nearest neighbour sites. However, inside segment 2, a new  $P$  particle (yellow circle) can attach only at  $i = L_1$ , with rate  $\alpha_q$ , only if this site is empty. Once attached, a  $P$  particle can hop forward only from left to right (i.e.  $i \rightarrow i + 1$ ) by a single site in each step, with rate  $q$ , provided the target site is empty. Normally, a  $P$  particle would continue its hopping till it reaches the site  $L_2$  from where it detaches with rate  $\beta_q$ . Thus, the lattice sites in the segments 1 and 3 can be occupied by only the  $R$  particles, whereas a mixed population of  $R$  and  $P$  particles can exist in the segment 2.

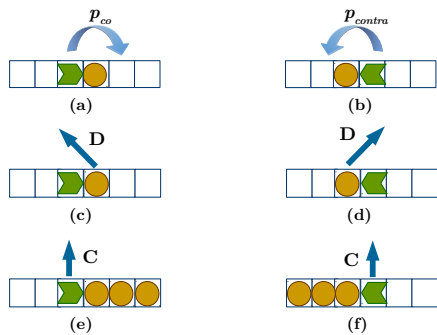


FIG. 2. Schematic representation of interference between the  $R$  particles and the  $P$  particles. In (a) and (b)  $R$  particle can pass the  $P$  particle, with rates  $p_{co}$  and  $p_{contra}$ . In (c) and (d) the  $R$  particle can knock the  $P$  particle out of the track, with rate  $D$ . In (e) and (f)  $P$  particle can block the progress of the  $R$  particle thereby causing its eventual collapse, with rate  $C$ .

continues hopping until it reaches a nearest neighbor of that particular site of stall or collapse, it also indicates successful completion of replication and, therefore, identified as a successful event of type 2 (from now onwards, referred to as sr2). But if both the  $R$  particles are stalled (i.e., replication fork collapsed) before completely covering the entire lattice together by hopping between the sites 1 and  $L$ , then the process is identified as unsuccessful event (usr). Dividing the sum total of the times taken

by all the sr1 and sr2 events by the total number of all such events we obtain the mean hopping time of a  $R$  particle ( $\tau$ ), which is the mean time required for successful completion of replication of the DNA of length  $L$  (in the units of “base pairs”).

### III. RESULTS

Although our model captures just a few key aspects of the biological processes involved in the transcription-replication conflict, the proposed model is already too complex to allow a rigorous analytical treatment. We therefore rely mainly on Monte Carlo (MC) simulations. However, in certain limiting situations, the computer simulations are complemented by an approximate analytical theory, that draws heavily on the known exact results for TASEP with single species of particles. The transparent arguments of the analytical derivations provide some insight into the underlying physical processes. However, the analytical derivation is based primarily on heuristic arguments some steps of which are essentially equivalent to mean-field approximations. Therefore, the accuracy of our heuristic analytical arguments have been checked by comparison with the corresponding data obtained from the MC simulations.

In the MC simulations we adopted random sequential updating to investigate the effects of traffic of  $P$  particles on the kinetics of  $R$  particles, i.e, the effects of ongoing transcription on replication. The data collected during the simulations are averaged over 10000 realizations each starting from a fresh initial configuration. We convert the rates into probabilities by using the conversion formula  $p_k = k dt$  where,  $k$  is an arbitrary rate constant and  $dt$  is an infinitesimally small time interval; the typical numerical value of  $dt$  used in our simulations is  $dt = 0.001 s$ . Unless stated explicitly otherwise, the numerical values of the relevant parameters used in the simulations are  $L = 2000$ ,  $L_1 = 500$ ,  $L_2 = 1500$ ,  $B_1 = B_2 = 300 s^{-1}$ ,  $\beta_q = 1000 s^{-1}$  and  $q = 30 s^{-1}$ .

#### A. Effects of steady traffic of RNA polymerases on replication time

The time needed for a successful completion of replication (now onwards, referred to as “replication time”) is identified as the time taken by the two  $R$  particles to meet head-on, starting from their simultaneous entry into the lattice through  $i = 1$  and  $i = L$ . In order to measure the replication time in the steady traffic of  $P$  particles in the MC simulations, we first switch on the entry of only the  $P$  particles (i.e., transcription) through  $i = L_1$ . The two  $R$  particles are allowed to enter simultaneously, through  $i = L_1$  and  $i = L_2$  only after the flux of the  $P$  attains its constant value in the non-equilibrium steady-state of the TASEP. Once the  $R$  particles enter the segment 2 and start encountering the  $P$  particles, the rate of replication

begins to get affected adversely.

We first present the derivation of the analytical results before comparing with the corresponding data obtained from MC simulation. Suppose  $n$  denotes the number of particles in the segment 2 of the lattice. In the limit  $n \gg 1$ , the effects of a single  $R$  particle on the flow of the  $P$  particles is expected to be negligibly small so that the movement of the  $P$  particles can be approximated well by a purely single-species TASEP in the segment 2. Under this assumption, the flux  $J_P$  of the  $P$  particles corresponding to the number density  $\rho$  inside segment 2 is given by the standard formula (see, for example, [54])

$$J_P = q\rho(1 - \rho). \quad (1)$$

Since, because of the open boundaries,  $n$  fluctuates with time even in the steady state, the number density  $\rho = n/(L_2 - L_1)$ , also fluctuates with time. The effective velocity of the  $P$  particles corresponding to the flux (1) in segment 2 is given by,

$$v_P = \frac{J_P}{\rho} = q(1 - \rho). \quad (2)$$

First we explore the parameter regime where  $\beta$  is so large that at sufficiently low values of  $\alpha$  the  $P$  particles would be in the low-density (LD) phase of the TASEP (in the ‘‘initiation’’-limited regime in the terminology of transcription). With the increase of  $\alpha$  the system would make a transition to the maximal current (MC) phase of TASEP (‘‘elongation-limited’’ regime of transcription). For the analytical derivation, we assume the following simplified situations:

- (a) None of the  $R$  particles collapse (i.e.  $C = 0$ ) upon encounter with  $P$  particles,
- (b) None of the  $R$  particles can detach from the lattice prematurely (i.e.  $D = 0$ ),
- (c) In the absence of any hindrance, the rate of replication by both the forks are identical, i.e., the symmetric case:  $B_1 = B_2 = B$ .

Since the time intervals between the entry of the  $P$  particles at  $i = L_1$  is quite long, the number of  $P$  particles encountered co-directionally by  $R_\ell$  and that head-on by  $R_r$  would be almost identical under the conditions (a)-(c) above, the most-probable location for the head-on meet of the two oppositely moving  $R$  particles is expected to be the midpoint of the segment 2 (i.e. at  $i, i + 1 \approx L/2, L/2 \pm 1$ ), and

- (d) In order to simplify the analytical expressions, we also assume that the length of the segment 2 is  $\approx L/2$ .

Let us define

$$\frac{\alpha q}{q} \rightarrow \alpha, \quad \frac{\beta q}{q} \rightarrow \beta. \quad (3)$$

as the rescaled initiation and termination rates, respectively, of a  $P$  particle. Using the well known results for the flux and density profile of TASEP under open boundary conditions [55, 56], we get expressions for  $J_2$  and

$v_2$ , in all three possible phases: In the low density (LD) phase,

$$J_P = q\alpha(1 - \alpha), \quad v_P = q(1 - \alpha), \quad (4)$$

in the high density (HD) phase,

$$J_P = q\beta(1 - \beta), \quad v_P = q(1 - \beta), \quad (5)$$

and in the maximal current (MC) phase,

$$J_P = \frac{q}{4}, \quad v_P = \frac{q}{2}. \quad (6)$$

Next, we define the effective velocity of a  $R$  particle inside segment 2. For  $R_\ell$

$$v_{R_\ell} = \begin{cases} B_1(1 - \rho) & \text{if no P particle in front} \\ p_{\text{co}}(1 - \rho) & \text{if P particle is in front} \end{cases} \quad (7)$$

whereas for  $R_r$

$$v_{R_r} = \begin{cases} B_2(1 - \rho) & \text{if no P particle in front} \\ p_{\text{contra}}(1 - \rho) & \text{if P particle is in front} \end{cases} \quad (8)$$

Therefore, the relative velocities  $v_r$  with which a  $R$  particle approaches a leading  $P$  particle, are  $v_{R_\ell} - v_P$  and  $v_{R_r} + v_P$  for co-directional and contra-directional encounter, respectively. The average separation  $d$  between the  $P$  particles, i.e., distance headway between the successive particles, in the segment 2 is

$$d = \frac{1}{\rho}. \quad (9)$$

From expressions (2), (7) and (8), the average interaction times  $\tau_{\text{co}}$  and  $\tau_{\text{contra}}$ , between a  $R$  particle and a  $P$  particle, during co-directional and contra-directional encounter, are given by,

$$\begin{aligned} \tau_{\text{co}} &= \frac{d}{v_{R_\ell} - v_P} \\ &= \frac{1}{2\rho} \left[ \frac{1}{B_1(1 - \rho) - q(1 - \rho)} + \frac{1}{p_{\text{co}}(1 - \rho) - q(1 - \rho)} \right], \end{aligned} \quad (10)$$

and

$$\begin{aligned} \tau_{\text{contra}} &= \frac{d}{v_{R_r} + v_P} \\ &= \frac{1}{2\rho} \left[ \frac{1}{B_2(1 - \rho) + q(1 - \rho)} + \frac{1}{p_{\text{co}}(1 - \rho) + q(1 - \rho)} \right]. \end{aligned} \quad (11)$$

where we have arrived at the expression for  $\tau_{\text{co}}$  assuming it to be an average of the contributions from the two situations mentioned in (7). Similarly the expression for  $\tau_{\text{contra}}$  is also the average of the two contributions from the alternative cases mentioned in (8).

Next, we define  $N_{\text{co}}$  and  $N_{\text{contra}}$ , as the total number of encounters that a  $R$  particle can suffer inside the segment 2. We derive approximate expressions for  $N_{\text{co}}$  and  $N_{\text{contra}}$ . When the conditions (a)-(d) are satisfied,  $N_{\text{co}}$  and  $N_{\text{contra}}$  are given by the expressions

$$N_{\text{co}} = N_{\text{contra}} \approx \frac{\rho L}{4}. \quad (12)$$

where the factor  $L/4$  arises from the fact that each of the  $R$  particles has to traverse a distance of  $L/4$  to reach the middle of the segment 2. From expressions (10), (11) and (12), we calculate the total hopping time of a  $R$  particle inside segment 2, i.e.  $\tau_{\text{int}}$ , as a product of total number of interactions and average encounter time. In the steady state,  $\tau_{\text{int}}$  is given by

$$\begin{aligned} \tau_{\text{int}} &= N_{\text{co}} \tau_{\text{co}} + N_{\text{contra}} \tau_{\text{contra}} \\ &= \frac{\rho L}{4} (\tau_{\text{co}} + \tau_{\text{contra}}). \end{aligned} \quad (13)$$

Further, we calculate the total replication time  $\tau$  as a summation of replication times inside segment 1 and 3 and replication time  $\tau_{\text{int}}$  inside segment 2,

$$\begin{aligned} \tau &= \frac{\tau_{\text{int}}}{2} + \frac{L}{4B_1} \\ &= \frac{\rho L}{8} (\tau_{\text{co}} + \tau_{\text{contra}}) + \frac{L}{4B_1}, \end{aligned} \quad (14)$$

where the extra factor of  $1/2$  in the first term on the right hand side is needed to average over the two directions of encounter. Note that the dependence of  $\tau$  on  $\alpha_q$  arises in (14) from the use of the result  $\rho(\alpha) = \alpha$  for the LD phase of  $P$  particles where the relation between  $\alpha$  and  $\alpha_q$  is given by (3).

In Fig. 3, we show the variation of replication time  $\tau$  with the rate of transcription initiation (i.e., entry rate  $\alpha_q$  of the  $P$  particles), for a constant transcription termination rate (exit rate of  $P$  particles)  $\beta_q$ . With the increase of  $\alpha_q$ ,  $\tau$  increases, and eventually saturates, above a critical value of  $\alpha_q$ . This behavior is qualitatively reproduced by the heuristic analytical arguments. The latter, however, tends to slightly overestimate the mean replication time.

The steady state density profiles of the  $P$  particle are plotted in the inset of Fig. 3 for few different values of  $\alpha_q$ . The trend of variation of the profiles with  $\alpha_q$  is consistent with the transition from the LD phase to MC phase of the TASEP of the  $P$  particles. For all those values of  $\alpha_q$ , for which system is in LD phase, particle density  $\rho$  increases with increase of  $\alpha_q$ . Therefore, the total number of encounters that a  $R$  particle can have inside segment 2 also increases, which results the increase in  $\tau$ . Above a critical value of  $\alpha_q$ , the TASEP in the segment 2 makes a transition to the MC phase where the number density  $\rho$  of the  $P$  particles and, hence,  $\tau$ , becomes independent of  $\alpha_q$ .

In Fig. 3 we have plotted  $\tau$  against  $\alpha_q$  for two distinct cases. In the first  $p_{\text{co}} = p_{\text{contra}} = 30 \text{ s}^{-1}$  (i.e., the rates of

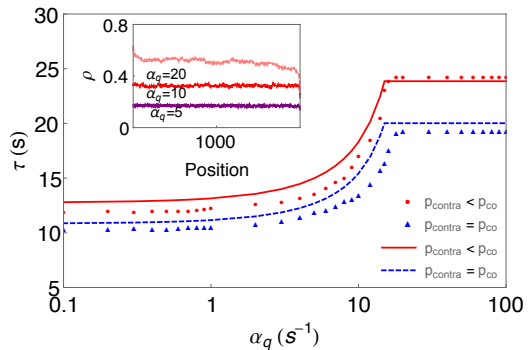


FIG. 3. Variation in average hopping time ( $\tau$ ) is plotted with  $\alpha_q$ , for two different sets of values of  $p_{\text{co}}$  and  $p_{\text{contra}}$ . In first case,  $p_{\text{co}} = p_{\text{contra}} = 30 \text{ s}^{-1}$  and in second case  $p_{\text{co}} = 30 \text{ s}^{-1}, p_{\text{contra}} = 20 \text{ s}^{-1}$ . Our theoretical predictions, based on heuristic analytical arguments, are drawn by continuous curves and numerical data obtained from our MC-simulations are shown by discrete points. In inset, we plot the density profile of  $P$  particles along the lattice, for three different values of  $\alpha_q$ . The density profile data have been obtained only from MC simulations. The other relevant model parameters are  $\beta_q = 1000 \text{ s}^{-1}, q = 30 \text{ s}^{-1}, C = D = 0 \text{ s}^{-1}$ .

passing is same irrespective of the direction of encounter). But in the second case rates of passing are asymmetric, i.e.,  $p_{\text{contra}} < p_{\text{co}}$ , where  $p_{\text{co}} = 30 \text{ s}^{-1}$  and  $p_{\text{contra}} = 20 \text{ s}^{-1}$ . The lower value of  $\tau$  in the latter case shows that even if one of the passing rates decreases, it leads to a lowering of the time needed for completion of replication because a  $R$  particle has to pause for longer duration.

Next, based on similar heuristic mean-field-type arguments, we derive analytical expressions for the average replication time in the opposite limit where  $\alpha$  is sufficiently high. In this parameter regime, at sufficiently small values of  $\beta$ , the system is in the high density (HD) phase of TASEP (“termination”-limited regime of transcription), but makes a transition to the MC phase with the increase of  $\beta$ . For the analytical arguments, we assume the same special scenario (a)-(c) above, i.e.,  $C = 0 = D$  and  $B_1 = B_2 = B$ .

In this case, because of the high value of  $\alpha$  the particle  $R_r$  is expected to suffer large number of encounters with  $P$  particles all of which approach it head-on. Even if it succeeds entering the segment 2 through  $i = L_2$  and move ahead at a slow pace by passing oncoming  $P$  particles, new  $P$  particles continue to make fresh entries into this segment through  $i = L_1$ . Thus, the number of particles to be bypassed by  $R_r$  keep increasing as time passes till  $R_r$  exits the segment 2 through  $i = L_1$ . In contrast, the particle  $R_\ell$  encounters far fewer  $P$  particles because, after it enters the segment 2, the new entrant  $P$  particles would be falling behind it and even some of those in front would make their exit from  $i = L_2$  before  $R_\ell$  catches up co-directionally from behind. Therefore, we make the simplifying assumption (perhaps, slight oversimplification) that the particle  $R_r$  remains stalled at

$i = L_2 + 1$  and replication is completed only when  $R_L$  reached  $i = L_2$ .

The average number of  $P$  particles within the segment from  $L_1$  to  $L_2$  is  $(L_2 - L_1)\rho$  where  $\rho$  is the average number density of the  $R$  particles in this segment. The average spatial gap between the  $P$  particles, as given by eq. (9), is  $1/\rho$  and the number of gaps to be covered by a  $R$  particle is  $(L_2 - L_1)\rho$ . Therefore, the total time spent by the  $R$  particle in exchanging its position with the co-directionally moving  $P$  particles is

$$\tau_{\text{exch}} = (L_2 - L_1)\rho/p_{\text{co}}. \quad (15)$$

The effective velocity of a  $R$  particle in the segment between  $L_2$  and  $L_1$  is  $B - q$ . The total time spent by the  $R$  particle in covering all the gaps by forward hopping is

$$\tau_{\text{hop}} = (L_2 - L_1)\rho \frac{1}{\rho(B - q)} = (L_2 - L_1)/(B - q). \quad (16)$$

The time taken by the  $R$  particle to reach  $L_1$  from  $i = 1$  is

$$\tau_{\text{arr}} = L_1/B. \quad (17)$$

Thus, finally, the total time taken to complete replication is

$$\tau = \frac{(L_2 - L_1)\rho}{p_{\text{co}}} + \frac{(L_2 - L_1)}{(B - q)} + \frac{L_1}{B}. \quad (18)$$

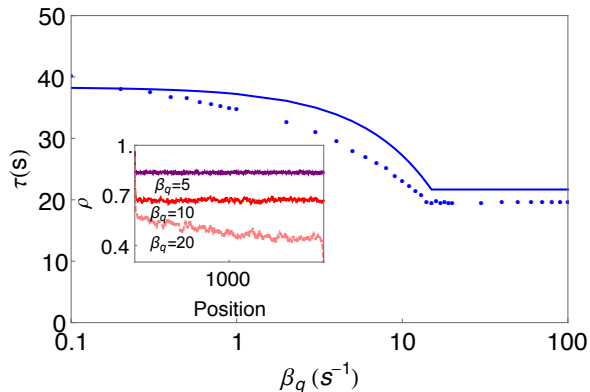


FIG. 4. The replication time  $\tau$  is plotted as a function of  $\beta_q$ . Our theoretical predictions, based on heuristic analytical arguments, are drawn by continuous curves and numerical data obtained from our MC-simulations are shown by discrete points. In inset, we plot the density profile of  $P$  particles along the lattice, for three different values of  $\beta_q$ . The density profile data have been obtained only from MC simulations. The other relevant model parameters are  $\alpha_q = 100\text{s}^{-1}$ ,  $q = 30\text{s}^{-1}$ ,  $p_{\text{co}} = p_{\text{contra}} = 30\text{s}^{-1}$ .

In Fig. 4, we show the variation of replication time  $\tau$  with the rate of transcription termination (i.e., exit rate  $\beta_q$  of the  $P$  particles), for a constant transcription initiation rate (entry rate of  $P$  particles)  $\alpha_q$ . Note that

the dependence of  $\tau$  on  $\alpha_q$  arises in (18) from the use of the result  $\rho(\beta) = 1 - \beta$  for the HD phase of  $P$  particles where the relation between  $\beta$  and  $\beta_q$  is given by (3). With the increase of  $\beta_q$ ,  $\tau$  decreases, and eventually saturates, above a critical value of  $\beta_q$ . This behavior is qualitatively reproduced by the heuristic analytical arguments which slightly overestimate the mean replication time. The steady state density profiles of the  $P$  particle are plotted in the inset of Fig. 4 for few different values of  $\beta_q$ . The trend of variation of the profiles with  $\beta_q$  is consistent with the transition from the HD phase to MC phase of the TASEP of the  $P$  particles. For all those values of  $\beta_q$ , for which system is in HD phase, particle density  $\rho$  decreases with increase of  $\beta_q$ . Therefore, the total number of encounters that a  $R$  particle can have inside segment 2 also decreases, which results the decrease in  $\tau$ . Above a critical value of  $\beta_q$ , the TASEP in the segment 2 makes a transition to the MC phase where the number density  $\rho$  of the  $P$  particles and, hence,  $\tau$ , becomes independent of  $\beta_q$ .

In the absence of collapse of the replication fork ( $C = 0$ ) and premature detachment of RNAP ( $D = 0$ ), the replication time is essentially decided by the density of the RNAP motors (i.e.,  $R$  particles). Since one or two  $R$  particles make hardly any noticeable perturbation of the density that is prescribed by the exact theory for a pure TASEP of  $P$  particles, the expressions (14) and (18) for the replication time  $\tau$  are in excellent agreement with the corresponding data obtained from MC simulation of the model.

## B. Histograms of the Number of Successful and Unsuccessful Replication Events

In this subsection we show the effects of transcription on replication. For this purpose, we calculate how the distributions of the three processes, namely, sr1, sr2 and usr are affected by the encounter of  $R$  particles with the  $P$  particles.

### • Special case of $C \neq 0$ and $D = 0$

Nonzero  $C$  gives rise to two other alternative scenarios. If only one of the  $R$  particles collapses and the other does not replication is completed via the alternative route that we defined as sr2. Similarly, collapse of both the  $R$  particles leads to nonzero probability of usr. Note that any increase in the probabilities of sr2 or usr, or both, cause reduction in the probability of sr1 because  $P_{\text{sr1}} + P_{\text{sr2}} + P_{\text{usr}} = 1$ .

Suppose, on the average, the total number of  $P$  particles in the segment between  $i = L_1$  and  $i = L_2$  is  $N$ . If  $N$  events of passing in the segment between  $i = L_1$  and  $i = L_2$  is required for completion of replication without suffering collapse of either of the two replication forks,

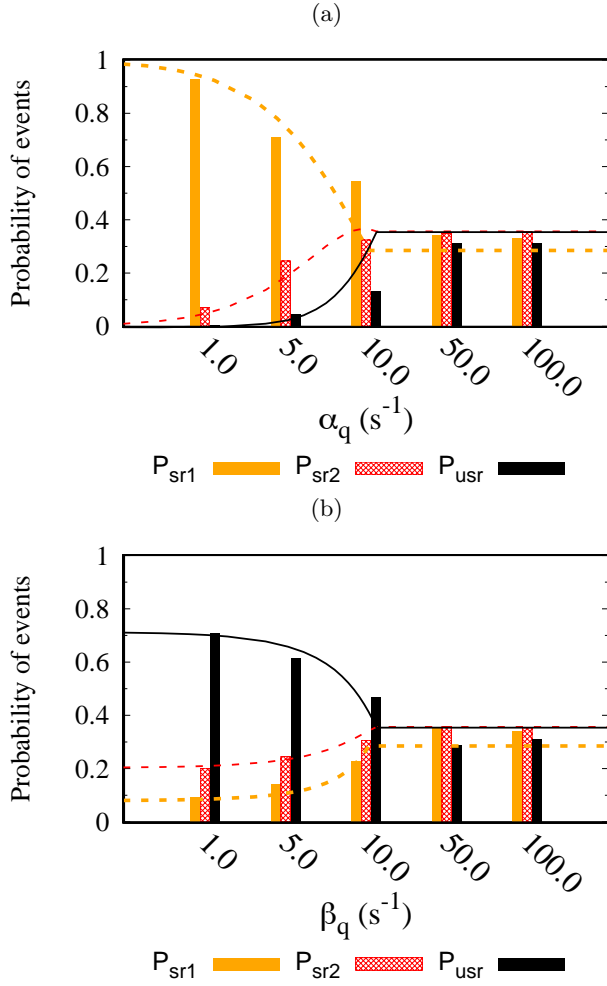


FIG. 5. Distribution of sr1, sr2 and usr in the special case  $C \neq 0$ ,  $D = 0$  is plotted for five different values of (a)  $\alpha_q$ , for fixed  $\beta_q = 1000 \text{ s}^{-1}$  and (b)  $\beta_q$ , for fixed  $\alpha_q = 1000 \text{ s}^{-1}$ . The data used for the bar plots have been obtained by MC-simulations. Lines have been obtained from the analytical expressions (19), (20) and (21). Dotted line corresponds to  $P_{\text{sr1}}$ , dashed line corresponds to  $P_{\text{sr2}}$  and continuous line corresponds to  $P_{\text{usr}}$ . The other relevant parameters used in this figure are  $L = 2000$ ,  $q = 30 \text{ s}^{-1}$ ,  $C = 0.05 \text{ s}^{-1}$ ,  $D = 0$  and  $p_{\text{co}} = p_{\text{contra}} = p = 20 \text{ s}^{-1}$ .

then the probability of sr1 is

$$P_{\text{sr1}} = \left( \frac{p}{p+C} \right)^N \quad (19)$$

For sr2, one of the forks ( $R$  particles) has to collapse while the remaining stretch of the segment between  $i = L_1$  to  $i = L_2$  is covered by the surviving fork. One of the forks may collapse after passing  $n$  number of  $P$  particles; the probability of its occurrence is  $[C/(p+C)][p/(p+C)]^n$ ; the probability that the surviving fork passes the other remaining  $P$  particles is  $[p/(p+C)]^{N-n}$ . Thus, the

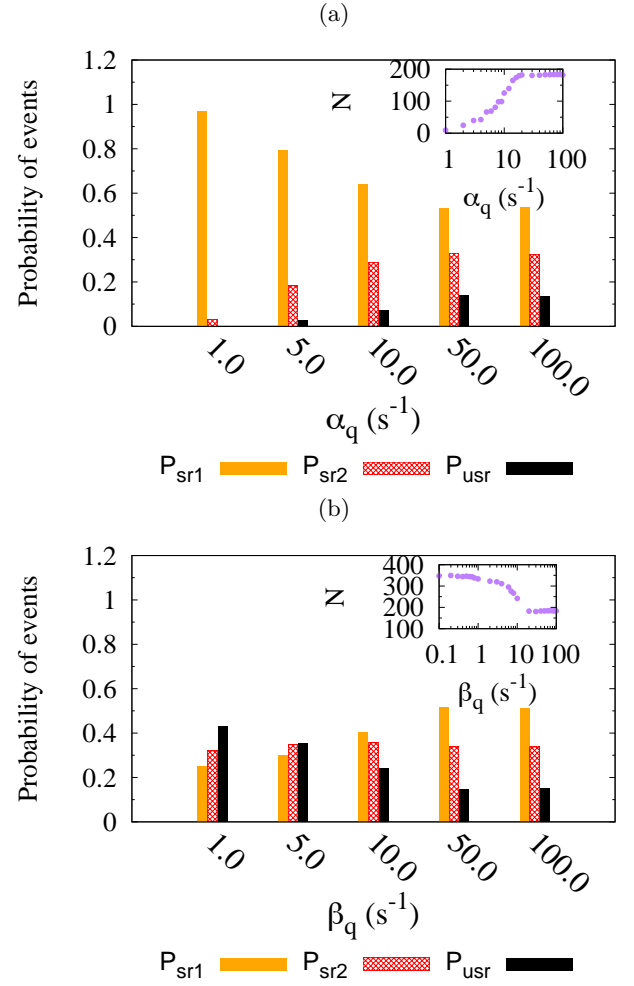


FIG. 6. Distribution of sr1, sr2 and usr in the general case  $C \neq 0$ ,  $D \neq 0$  is plotted for five different values of (a)  $\alpha_q$ , for fixed  $\beta_q = 1000 \text{ s}^{-1}$  and (b)  $\beta_q$ , for fixed  $\alpha_q = 1000 \text{ s}^{-1}$ . In inset we plot the variation in  $N$  (i.e. average number of  $P$  particle detached from the track during their encounter with  $R$  particles) with (a)  $\alpha_q$  and (b)  $\beta_q$ . These data have been obtained only from MC-simulations. The other relevant parameters used in this figure are  $L = 2000$ ,  $q = 30 \text{ s}^{-1}$ ,  $C = 0.05 \text{ s}^{-1}$ ,  $D = 10 \text{ s}^{-1}$  and  $p_{\text{co}} = p_{\text{contra}} = p = 20 \text{ s}^{-1}$ .

probability of sr2 is

$$\begin{aligned} P_{\text{sr2}} &= \sum_{n=0}^{N-1} \left[ \left( \frac{C}{p+C} \right) \left( \frac{p}{p+C} \right)^n \right] \left( \frac{p}{p+C} \right)^{N-n} \\ &= N \left( \frac{C}{p+C} \right) \left( \frac{p}{p+C} \right)^N \end{aligned} \quad (20)$$

Exploiting normalization, we get the probability for usr

$$P_{\text{usr}} = 1 - P_{\text{sr1}} - P_{\text{sr2}}. \quad (21)$$

Note that  $N = \rho(L_2 - L_1)$  is the average number of  $P$  particles in the interaction segment between  $i = L_1$  and  $i = L_2$ . In the LD regime of  $P$  particles  $\rho = \alpha = \alpha_q/q$ .

In Fig. 5, we plot the distributions of 'sr1', 'sr2' and 'usr' as histograms for (a) five distinct values of  $\alpha_q$  and a constant value of  $\beta_q$ , and (b) five distinct values of  $\beta_q$  and a constant value of  $\alpha_q$ . The analytic approximations (19)–(21) reproduce qualitatively the behavior observed in the MC simulations. For a given sufficiently high value of  $\beta_q$ , segment 2 is in the LD phase at small values of  $\alpha_q$ . In this regime the number of eventual collapse of a  $R$  particle during its encounters with  $P$  particles is negligibly small. Therefore, for these small values of  $\alpha_q$ , number of events of the type 'sr2' and 'usr' are low and, hence the probability of sr1 is very weakly affected (see Fig. 5(a)). As  $\alpha_q$  increases further, the number of eventual collapse increases because of the increasing number of encounters with  $P$  particles which is reflected in the significant increase in 'sr2' and 'usr' in Fig. 5(a). Increase in the probabilities of sr2 and usr results in the corresponding decrease in the probability of sr1 because of the normalization of the probabilities mentioned above. Number of the events 'sr1', 'sr2' and 'usr' attain their respective saturation values as  $\alpha_q$  increases above the critical value where the transition from LD phase to MC phase takes place (see Fig. 5(a)).

Similarly, for a sufficiently high value of  $\alpha_q$ , with increasing  $\beta_q$  the  $P$  particles exhibit a transition from the HD phase to the MC phase. Consequently, the decrease in the frequency of encounter of the  $P$  particles with the  $R$  particles. The likelihood of collapse of both the  $R$  particles in any run decreases as indicated by the increase of the probability of sr2. The concomitant increase of the probability of sr is also shown in Fig. 5(b).

#### • Special case of $C \neq 0$ and $D \neq 0$

Now, we consider the general case of our model allowing for the possibilities that  $C \neq 0$  and  $D \neq 0$ . As we have already done in the restricted case of  $C \neq 0$ ,  $D = 0$ , we characterize the effect of nonzero  $C$  and  $D$  also in terms of the statistics of 'sr1', 'sr2' and 'usr'.

In Fig. 6(a) and (b), we plot the distributions of the events 'sr1', 'sr2' and 'usr' as histograms for (a) five different values of  $\alpha_q$  at a constant high value of  $\beta_q$  and (b) five different values of  $\beta_q$  at a constant high value of  $\alpha_q$ . The trends of variation of these three probabilities are explained by the transition to the MC phase from (a) LD phase and (b) HD phase.

In the inset of Fig. 6, we display the effects of replication on transcription. We show the variation in the number  $N$  of  $P$  particles that detach from the lattice when they encounter a  $R$  particle, for a given rate  $\alpha_q$ . The trend of variation and the physical reason for this trend is also well explained by the transition from LD phase to MC phase.

### C. Distribution of Detachments of $P$ Particles

In MC simulations, we measure the time intervals between two consecutive  $P$  detachment events as  $\delta t_1, \delta t_2 \dots \delta t_n$ , if  $n+1$  detachments takes place in a single MC simulation run. Since this is a stochastic process these time intervals  $\delta t_1, \delta t_2 \dots \delta t_n$  are, in general, different from each other. We compute the number of consecutive  $P$  detachment events corresponding to a given interval  $\delta t$ , i.e. if two time intervals are identical ( $\delta t_i = \delta t_j = \delta t$ ), then, number of consecutive  $P$  detachment events with time interval  $\delta t$  is 2. We repeat the procedure over 10000 MC simulation runs to calculate total number of consecutive  $P$  detachment events with given interval  $\delta t$ , and then we divide this number with number of MC simulation runs, i.e. 10000, to calculate the average number  $N_\alpha$  of consecutive  $P$  detachments within the time interval  $\delta t$  for a fixed rate  $\alpha_q$ .

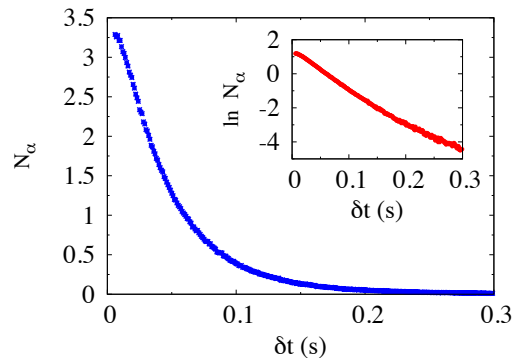


FIG. 7. Distribution of  $N_\alpha$  is plotted with  $\delta t$  for a constant  $\alpha_q = 100 \text{ s}^{-1}$ . In inset we plot  $N_\alpha$  with  $\delta t$  on a semi-log axis to show the exponential fall of  $N_\alpha$  with  $\delta t$ . These data have been obtained only by MC-simulations. The other relevant parameters used in this figure are  $C = 0.05 \text{ s}^{-1}$ ,  $D = 10 \text{ s}^{-1}$ ,  $p_{\text{co}} = 20 \text{ s}^{-1}$  and  $p_{\text{contra}} = 20 \text{ s}^{-1}$ .

In Fig. 7 we show the variation in  $N_\alpha$  with  $\delta t$  and we find that  $N_\alpha$  falls exponentially as the time interval between two consecutive  $P$  detachment events increases. To confirm the exponential behavior, in the inset we show the variation in  $N_\alpha$  on a semi-log axis with  $\delta t$ .

## IV. SUMMARY AND CONCLUSION

In this paper we have developed the first minimal model that captures the key kinetic rules for the resolution of conflict between transcription and concomitant replication of the same stretch of DNA. This model has been formulated in terms of a two-species exclusion process where one species of particles (denoted by  $P$ ) represents the RNA polymerase motors while the two members of the other species (denoted by  $R$ ) represent the two replication forks.



In contrast to all the multi-species exclusion models reported so far, the allowed populations of the two species are quite different in our model. A maximum of only two  $R$  particles are allowed to enter the lattice; imposition of this restriction on the number of  $R$  particles is motivated by the fact that none of the segments of DNA should be replicated more than once during the life time of a cell. In sharp contrast, the number of  $P$  particles is not restricted except for the control of their population by the rate constants for their entry, exit and hopping. This choice is consistent with the fact that the multiple rounds of transcription of the same segment of DNA is not only possible but resulting synthesis of multiple identical transcripts is also desirable for the proper biological function of the cell. Moreover, all the  $P$  particles move co-directionally, from left to right whereas one of the  $R$  particles (namely,  $R_\ell$ ) moves from left to right while the other  $R$  particle (namely  $R_r$ ) approaches it head-on from the opposite end. Another distinct feature of this model is that the lattice consists of three segments; the encounters of RNAP motors ( $P$  particles) with the replication fork ( $R$  particles) are confined within the middle segment (segment 2) whereas only the  $R$  particles can occupy the sites in the segments 1 and 3.

By a combination of analytical treatment, based on heuristic arguments, and Monte Carlo simulations we have analyzed the effects of the RNA polymerase motor traffic on the DNA replication and vice versa. More specifically, we have shown how the transition from the

Low-density phase to the Maximal Current phase and that from the high-density phase to the maximal Current phase of  $P$  traffic affects the not only the total time required for successful completion of replication but also how the statistics of the successful and unsuccessful replication events are also affected.

Any attempt of direct comparison between the theoretical predictions of our model with the experimental data may be premature at this stage. There are some important features of DNA replication in eukaryotic cells that we hope to incorporate in future extensions of our model. For example, even after two replication forks begin approaching each other head-on, new pairs of replication forks can nucleate in the unreplicated segment of the DNA in between the two. However, the price to be paid for more realistic and more detailed would be to sacrifice the possibility of analytical treatments even on the basis of heuristic arguments. Nevertheless, computer simulations would still provide some mechanistic insight into the causes and consequences of the transcription-replication conflict.

This work has been supported by J.C. Bose National Fellowship (DC), “Prof. S. Sampath Chair” Professorship (DC), by UGC Senior Research Fellowship (BM) and the German Science Foundation (DFG) under grant SCHA 636/8-2 (AS).

- 
- [1] B. Derrida: *Phys. Rep.* **301**, 65 (1998)
- [2] G.M. Schütz: *Integrable stochastic many-body systems*, in: *Phase Transitions and Critical Phenomena* **19**, 1 (2000), Ed. C. Domb and J L Lebowitz (London: Academic)
- [3] A. Schadschneider, D. Chowdhury, K. Nishinari: *Stochastic Transport in Complex Systems: From Molecules to Vehicles* (Elsevier, 2010)
- [4] K. Mallick, *Physica A* **418**, 17-48 (2015).
- [5] C.T. MacDonald, J.H. Gibbs, A.C. Pipkin: *Biopolymers* **6**, 1 (1968).
- [6] C. MacDonald and J. Gibbs, *Biopolymers*, **7**, 707 (1969).
- [7] A. Basu and D. Chowdhury, *Phys. Rev. E* **75**, 021902 (2007).
- [8] A. Garai, D. Chowdhury, D. Chowdhury and T.V. Ramakrishnan, *Phys. Rev. E* **80**, 011908 (2009).
- [9] R.K.P. Zia, J.J. Dong and B. Schmittmann, *J. Stat. Phys.* **144**, 405 (2011).
- [10] C. Lin, G. Steinberg and P. Ashwin, *J. Stat. Mech. Theor. Expt.* P09027 (2011).
- [11] P. Greulich, L. Ciandrini, R.J. Allen and M.C. Romano, *Phys. Rev. E* **85**, 011142 (2012).
- [12] D. Chowdhury, A. Garai and J.S. Wang, *Phys. Rev. E* **77**, 050902(R) (2008).
- [13] D. Oriola, S. Roth, M. Dogterom and J. Casademunt, *Nat. Commun.* **6**, 8025 (2015).
- [14] K.E.P. Sugden, M.R. Evans, W.C.K. Poon and N.D. Read, *Phys. Rev. E* **75**, 031909 (2007).
- [15] M.R. Evans, Y. Kafri, K.E.P. Sugden and J. Tailleur, *J. Stat. Mech. Theor. Expt.*, P06009 (2011).
- [16] Y. Chai, S. Klumpp, M.J.I. Müller and R. Lipowsky, *Phys. Rev. E* **80**, 041928 (2009).
- [17] M. Ebbinghaus and L. Santen, *J. Stat. Mech.: Theor. Expt.* P03030 (2009).
- [18] M. Ebbinghaus, C. Appert-Rolland and L. Santen, *Phys. Rev. E* **82**, 040901 (R) (2010).
- [19] S. Muhuri and I. Pagonabarraga, *Phys. Rev. E* **82**, 021925 (2010).
- [20] I. Neri, N. Kern and A. Parmeggiani, *Phys. Rev. Lett.* **107**, 068702 (2011).
- [21] I. Neri, N. Kern and A. Parmeggiani, *Phys. Rev. Lett.* **110**, 098102 (2013).
- [22] I. Neri, N. Kern and A. Parmeggiani, *New J. Phys.* **15**, 085005 (2013).
- [23] A.I. Curatolo, M.R. Evans, Y. Kafri and J. Tailleur, *J. Phys. A: Math. Theor.* **49**, 095601 (2016).
- [24] S. Klein, C. Appert-Rolland and M.R. Evans, *J. Stat. Mech.* 093206 (2016).
- [25] A. Parmeggiani, T. Franosch and E. Frey, *Phys. Rev. E* **70**, 046101 (2004).
- [26] I.R. Graf and E. Frey, *Phys. Rev. Lett.* **118**, 128101 (2017).
- [27] D. Chowdhury, A. Schadschneider and K. Nishinari: *Phys. Life Rev.* **2**, 318 (2005).
- [28] T. Chou, K. Mallick and R.K.P. Zia: *Rep. Prog. Phys.* **74**, 116601 (2011).

- [29] D. Chowdhury: Phys. Rep. **529**, 1-197 (2013).
- [30] C. Appert-Rolland, M. Ebbinghaus and L. Santen: Phys. Rep. **593**, 1 (2015).
- [31] A.B. Kolomeisky: *Motor proteins and molecular motors*, (CRC Press, 2015).
- [32] A. Kornberg and T. Baker: *DNA Replication* (University Science Books, 1992).
- [33] T. Tripathi and D. Chowdhury: Phys. Rev. E **77**, 011921 (2008).
- [34] S. Klumpp and T. Hwa: Proc. Natl. Acad. Sci. **105**, 18159 (2008).
- [35] S. Klumpp: J. Stat. Phys. **142**, 1252 (2011).
- [36] M. Sahoo and S. Klumpp: EPL **96**, 60004 (2011).
- [37] Y. Ohta, T. Kodama and S. Ihara: Phys. Rev. E **84**, 041922 (2011).
- [38] J. Wang, B. Pfeuty, Q. Thommen, M.C. Romano and M. Lefranc: Phys. Rev. E **90**, 050701(R) (2014).
- [39] S. Jun, H. Zhang and J. Bechhoefer: Phys. Rev. E **71**, 011908 (2005).
- [40] S. Jun and J. Bechhoefer: Phys. Rev. E **71**, 011909 (2005).
- [41] J. Bechhoefer and B. Marshall: Phys. Rev. Lett. **98**, 098105 (2007).
- [42] S.C. Yang and J. Bechhoefer: Phys. Rev. E **78**, 041917 (2008).
- [43] A. baker, B. Audit, S.C.H. Yang, J. Bechhoefer and A. Arneodo: Phys. Rev. Lett. **108**, 268101 (2012).
- [44] R. Retkute, C. A. Nieduszynski, A. de Moura: Phys. Rev. Lett. **107**, 068103 (2011).
- [45] R. Retkute, C. A. Nieduszynski, A. de Moura: Phys. Rev. E **86**(3), 031916 (2012).
- [46] S.C. Yang, M.G. Gauthier and J. Bechhoefer: in *Methods in Mol. Biol., DNA Replication, vol. 521*, eds. S. Vengrova and J.Z. Dalggaard, (Springer 2009).
- [47] O. Hyrien and A. Goldar: Chromosome Research **18**, 147 (2010).
- [48] N. Kim and S. Jinks-Robertson, Nat. Rev. Genet. **13**, 204 (2012).
- [49] H. Merrikh, Y. Zhang, A.D. Grossman and J.D. Wang: Nat. Rev. Microbiol. **10**, 449 (2012).
- [50] A. Helmrich, M. Ballarino, E. Nudler and L. Tora: Nat. Struct. Mol. Biol. **20**, 412 (2013).
- [51] T. Garcia-Muse and A. Aguilera: Nat. Rev. Mol. Cell Biol. **17**, 553 (2016).
- [52] R. T. Pomerantz, M. O'Donnell: Cell Cycle (Georgetown, Tex.) **9**(13), 2537-2543 (2010).
- [53] A. Parmeggiani, T. Franosch, E. Frey: Phys. Rev. Lett. **90**, 086601 (2003).
- [54] D. Chowdhury, L. Santen, A. Schadschneider: Phys. Rep. **329**, 199 (2000).
- [55] B. Derrida, M.R. Evans, V. Hakim, V. Pasquier: J. Phys. A: Math. Gen. **26**, 1493 (1993)
- [56] G.M. Schütz, E. Domany: J. Stat. Phys. **72**, 277 (1993)
- [57] B. Liu, B.M. Alberts: Science **267**, 1131-1137 (1995)
- [58] P. Soutanas, Transcription **2:3**, 140 (2011).
- [59] S. French: Science **258**, 1362 (1992)
- [60] E.V. Mirkin and S.M. Mirkin: Microbiology and Molecular Biology Reviews **71**, 13-35 (2007)
- [61] R. Rothstein, B. Michel, S. Gangloff: Genes Development **14**, 110 (2000)